Multi-Machine Experiments to Study the Parametric Dependences of Momentum Transport and Intrinsic Torque

T. Tala[1], C. Chrystal[2], R.M. McDermott[3], S-P. Pehkonen[1], A. Salmi[1], C. Angioni[3], M. Barnes[4], B. Duval[5], C. Giroud[6], B. Grierson[7], W. Guttenfelder[7], J. Ferreira[8], J. Hillesheim[6], S. Kaye[7], P. Mantica[9], M.Maslov[6], S. Menmuir[6], F. Parra[4], C. Petty[2], T. Pütterich[3], J.E. Rice[10], F. Ryter[3], W. Solomon[7], G. Tardini[3], M.Tsalas[11], H.Weisen[5], M. Yoshida[12], JET contributors*, the ASDEX-Upgrade team, the DIII-D team, the NSTX team, the EUROfusion MST1 Team** and the ITPA Transport & Confinement Topical Group

EUROfusion Consortium, JET, Culham Science Centre, Abingdon, OX14 3DB, UK
[1]VTT, P.O. Box 1000, FIN-02044 VTT, Finland
[2]General Atomics, San Diego, US
[3]Max-Planck-Institut für Plasmaphysik, Boltmannstr. 2, 85748 Garching, Germany
[4]University of Oxford, Oxford, UK
[5]SPC, EFPL, Lausanne, Switzerland
[6]CCFE, Culham Science Centre, Oxon. OX14 3DB, United Kingdom
[7]Princeton Plasma Physics Laboratory, Princeton University, Princeton, New Jersey 08543, USA
[8]IST, Instituto de Plasmas e Fusao Nuclear, 1049-001 Lisbon, Portugal
[9]Istituto di Fisica del Plasma, via Cozzi 53, 20125 Milano, Italy
[10]MIT Plasma Science and Fusion Center, Cambridge, MA, USA
[11]DIFFER, Nieuwegein, Netherlands,
[12]Japan Atomic Energy Agency, Naka, Ibaraki-ken 311-0193, Japan
*See the Appendix of F. Romanelli et al., Proc. of the 25th IAEA Fusion Energy Conference 2014, St. Petersburg, Russia
**http://www.euro-fusionscipub.org/mst1 Email: tuomas.tala@vtt.fi

1. Introduction

Momentum transport and plasma rotation have been studied extensively on many tokamaks in recent years. Both experiments and theory have shown that sheared plasma rotation can stabilise turbulence while the rotation itself has beneficial effects on MHD instabilities, such as resistive wall modes. Future tokamaks, like ITER, will have larger moments of inertia and, therefore, less NBI torque per volume and less deep deposition profiles (NBI torque 'dominates' in present large tokamaks over other torque sources). Therefore, intrinsic torque will play a more important role in determining rotation for example in ITER.

Numerous experimental results, both on momentum transport and intrinsic torque, have been reported on individual devices – yet only few experimental multi-machine momentum transport or intrinsic torque comparisons have been performed. This paper reports dedicated scans to study momentum transport and intrinsic torque, carried out as dedicated joint experiments on JET, DIII-D, AUG, NSTX and C-Mod within the ITPA framework.

2. Multi-machine Experimental Scans of Momentum Transport

The NBI modulation experiments have been carried out in different types of plasmas to study parametric dependencies of momentum pinch (pinch number defined as $-R_0 v_{pinch}/\chi_\phi$) and Prandtl number (defined as $P_r=\chi_\phi/\chi_i$). The NBI modulation technique that creates a periodic rotation perturbation has been exploited on JET [1], DIII-D [2] and AUG [3]. In all AUG, JET and DIII-D experiments, the NBI torque was square wave modulated at a frequency f_{mod}=6.25Hz or f_{mod}=10Hz. This frequency is high enough to make the **J×B** torque the dominant source of torque perturbation outside r/a>0.3. The modulation cycle is, on the other hand, much longer than the time resolution of the Charge Exchange Recombination Spectroscopy (CXRS) diagnostic used to measure the toroidal rotation profile ω_ϕ and ion temperature T_i, the resolution varying from 2-10ms, depending on the device.

Time-dependent transport modelling of ω_ϕ by solving the full momentum transport equation is required to extract the transport properties from the plasma dynamic response, with the assumption that the time-dependent NBI torque can be calculated precisely with TRANSP. It is to be noted here that the NBI torque is the only source of torque taken into ac-

count in the analysis. Thus the following terms, which could affect the results presented in this paper, are neglected: residual stress $\Pi_{RS,}$ and possible torque sources/sinks due to MHD such as ELMs or NTMs and due to neo-classical toroidal viscosity. Only discharges without MHD or with only benign MHD were selected for further analysis. These terms will however appear in the determined intrinsic torque term that, in practice, thus consists of other torque sources from NBI. The analysis methodology in this study used to determine the momentum diffusivity and pinch is the similar to that described in [1,4], but further modified optimisation. The key thing in analysing these joint experiments is that the very same tools in using to analyse the data and determine the momentum transport coefficients (same settings, same tool to prepare experimental data for analysis), removing the possibility of uncertainties in the analysis results that often arise from employing different tools set across multi-tokamak data.

A 3-point dedicated collisionality υ^* scan was performed by varying collisionality by a factor of 4–5 while matching the other dimensionless profiles (ρ^*, β_N, q and T_i/T_e) on JET and DIII-D L-mode plasmas (JET and DIII-D had though different ρ^*, β_N, q, so not comparable to each other). The volume averaged ρ^* and β_N were matched to within 10%. The momentum pinch number does not depend on collisionality either on JET or on DIII-D as shown in figure 1 (middle frame). Similarly, the Prandtl number does not depend on υ^* either (left frame). However, it is to be noted that the momentum pinch numbers and the Prandtl numbers are higher on JET than on DIII-D. This could be due to different plasma parameters, i.e. JET has different values of ρ*, β or q than DIII-D. Or alternatively the intrinsic torque could play a different role in each device or the observed, larger, T_i modulation in JET is increasing effectively the Prandtl number more in JET than DIII-D [5]. On NSTX and AUG, such a dimensionless collisionality scan was not possible. However, it is possible to take data from pulses at nearly constant q and R/L_n, and these data have been included in figure 1 (right frame). No clear trend between the pinch number and υ* was found although the variation in υ* is small in AUG shots and the scatter in the data from NSTX is large. The error bars are challenging to estimate, typically they are around ±1 unit in the pinch number, but vary from pulse to pulse. There are several sources of error in the analysis, such input profile data, NBI torque, MHD affecting transport and two local minima close to each other found in the optimisation.

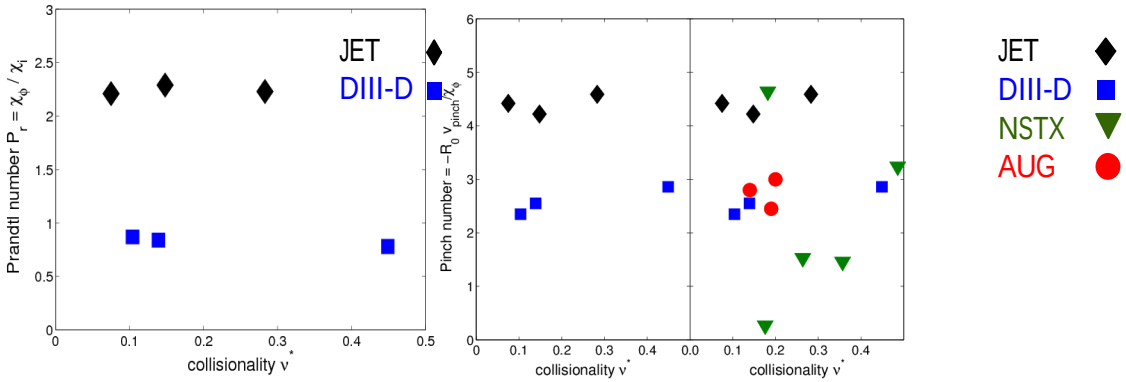

Figure 1. (Left frame) Prandtl number as a function of collisionality from the JET and DIII-D 3-point dimensionless collisionality scans. The data have been averaged between $0.5<\rho_{tor}<0.8$. (Middle frame) As in left frame, but for the pinch number. (Right frame) as in middle frame, but including data from AUG (red circles) and NSTX (green inverted triangles) pulses at almost constant q and R/L_n.

The dependence of the momentum pinch and Prandtl number on collisionality was also studied in linear gyro-kinetic simulations using the GS2 code. The GS2 runs were performed using the experimental data from each shot. The GS2 calculations were performed on a spectrum of 6 modes with k_y ranging from 0.15 to 0.8, with log spacing, This choice gives the usual peaking around $k_y\rho_i = 0.25$. In JET, neither momentum pinch nor the Prandtl number depends on collisionality, as shown in figure 2 (left frames). In DIII-D (right frames), the simulations tend to weakly suggest that both the Prandt and pinch numbers decrease with in-

creasing collisionality. However, in the inner region of the plasma (r/a<0.5) the observed dependence is in fact due to a smaller R/L_n in the high collisionality shot than due to a real collisionality dependence while in the outer half, R/L_n is matched well between the three shots.

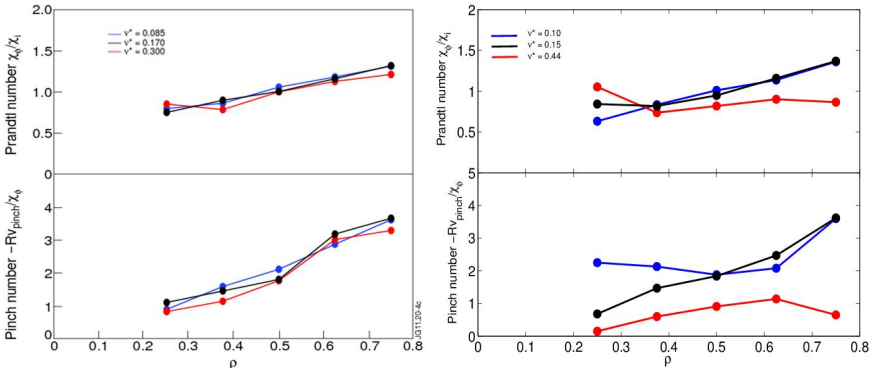

Figure 2. Prandtl number (upper frames) and pinch number (lower frames) profiles for the discharges forming the 3-point collisionality scan from linear GS2 simulations using the actual input data for JET shots (left) and DIII-D shots (right). The GS2 runs have been performed at five radial locations for each shot.

There is no simple way to perform a clean R/L_n scan in a tokamak without changing another dimensionless parameter simultaneously. In particular, the strong coupling between the collisionality and R/L_n in H-mode plasmas makes a R/L_n scan virtually impossible without changing the collisionality. However, since no dependence of momentum transport coefficients on collisionality was seen, it is possible to scan R/L_n by varying collisionality and assign the possible changes in momentum transport to R/L_n rather than collisionality. The dependence of the pinch number R_0v_{pinch}/χ_ϕ on R/L_n obtained from JET, DIII-D and AUG NBI modulation shots is illustrated in figure 3. It shows a clear dependence on R/L_n within the joint database, yielding $-Rv_{pinch}/\chi_\phi \approx 1.2R/L_n + 1.4$. The increase in the pinch number with increasing R/L_n is qualitatively consistent with Coriolis pinch theory and gyro-kinetic simulations [6].

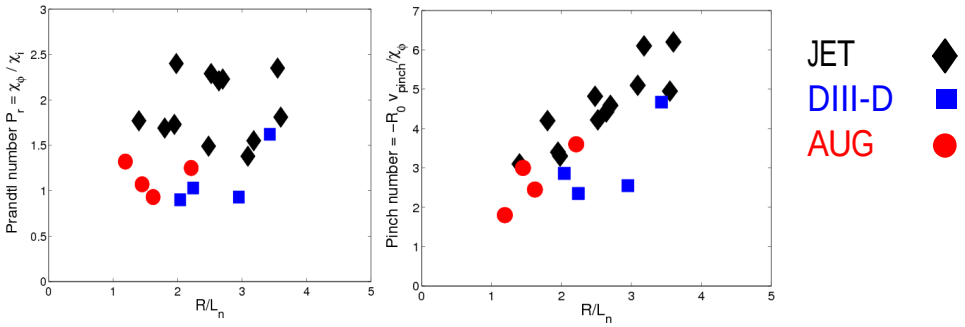

Figure 3. (Left frame) Prandtl numbers and (Right frame) pinch numbers as a function of the inverse density gradient length R/L_n from JET (black diamonds), DIII-D (blue squares) and AUG (red dots). The data have been averaged between $0.5<\rho_{tor}<0.8$. No trend in P_r on R/L_n is observed.

3. Multi-machine Experimental ρ* Scans to Study Intrinsic Torque

In order to study intrinsic torque, the most significant change in the experimental method was to reduce the modulation frequency of the NBI to 2-3Hz on each device. Here, two independent analysis methods were used; either so-called onion skin method [2] or by solving the full momentum transport equation using a $\chi_{\phi,eff}$ (no separate pinch) [7]. The dimensionless profiles (ρ^*, υ^*, β_N, q and T_i/T_e) are matched well (<10%) between the JET – AUG – DIII-D identity shot. The shape match between JET and DIII-D is good whereas the AUG shape is not perfectly match. In all machines, a successful match requires stretching operating far from each machine's comfort zone. The Mach number could not be matched whereas the gradient lengths are match well. The total integrated torque in figure 4 (left frame) is similar between the JET – AUG – DIII-D for the identity shot. While the total torque is similar between the

devices, their profiles are not although MHD is not playing in these shots. This may be due to the different way of analysing data, i.e. onion skin (JET, DIII-D) versus transport equation (AUG), up-down asymmetry being different in AUG, some other imperfection in the match. However, the most plausible reason is that another, unidentified quantity is playing a key role.

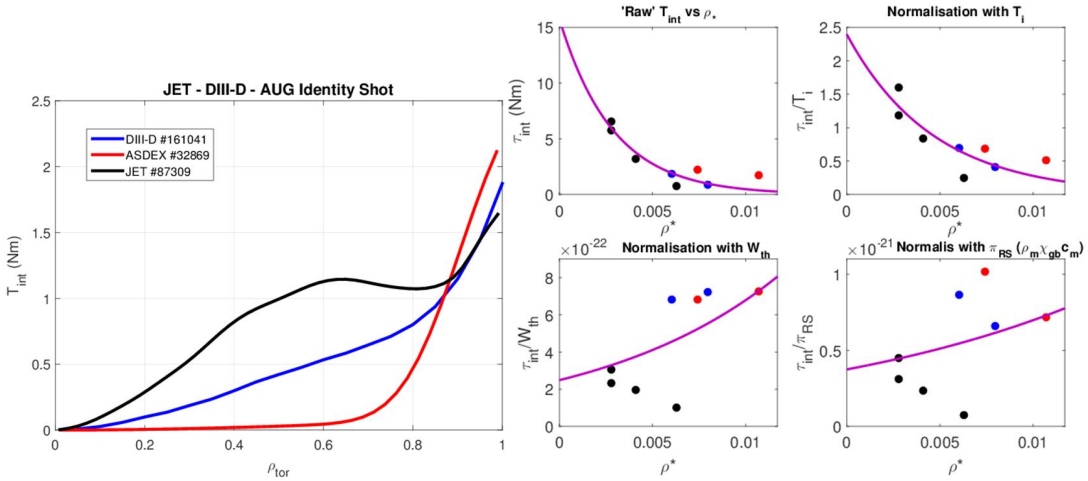

Figure 4. (Left frame) Integrated intrinsic torque for the multi-machine identity shot. (Right frame) Dimensionally matched ρ* scans from JET, DIII-D and AUG using different normalisation schemes. The solid lines represent the best fit to the multi-machine data.

Starting from the identity match discharges, three lower ρ* pulses from JET and one higher ρ* discharges from AUG and DIII-D [8] are added in the multi-machine ρ* dependence plots. All the other dimensionless parameters (υ*, β, q, R/L_n) are well-matched in this 8 point ρ* scan. The fit over different normalisations of the total integrated intrinsic torque, representing various ρ* scalings are shown in figure 4 (right frame). Now, there is no definite scientifically 'right' and widely-used way to normalise the torque, therefore different options are tested. Only T_i normalisation engenders a satisfying fit. The fit normalised with W_{th} and normalised with "residual stress", i.e. $\pi_{RS} = \rho_m \chi_{gb} c_s$ is poor. It also known that second derivatives may matter and those are obviously not matched. The key question, however, remains somewhat open, i.e. whether ρ* scaling of τ_{int} is positive or negative? This depends on the normalisation and so does ITER predictions for intrinsic torque – ranging from a few tens of Nm up to a few hundreds of Nm using this paper's ρ* scaling data set. To reduce the uncertainties for ITER predictions, more physics understanding other scaling experiments are needed.

4. Conclusions

Well matched dimensionless collisionality scans on JET and DIII-D showed no dependence of momentum transport on collisionality. The Prandtl number does not depend on inverse density gradient length. The pinch number shows a clear dependence on R/Ln in each device, with functional form $-Rv_{pinch}/\chi_\phi \approx 1.2R/L_n + 1.4$. The identity shot between JET – AUG – DIII-D shows about $\tau_{int} = 2$Nm for all devices. The deduced sign of ρ* scaling of intrinsic torque still depends on the applied normalisation. The most successful normalisation with Ti shows increasing τ_{int} with decreasing ρ*, to be tested against theory and modelling.

Acknowledgement: "This work has been carried out within the framework of the EUROfusion Consortium and has received funding from the Euratom research and training programme 2014-2018 under grant agreement No 633053. The views and opinions expressed herein do not necessarily reflect those of the European Commission." US Department of Energy with US Grant numbers from General Atomics (DE-FC02-04ER54698), Princeton Plasma Physics Laboratory (DE-AC02-09CH11466), and Massachusetts Institute of Technology (DE-FG02-94ER54235) are acknowledged.

[1] T. Tala et al., Phys. Rev. Lett. 102, 075001 (2009).
[2] W.M. Solomon et al., Phys. Plasmas 17, 056108 (2010).
[3] R.M. McDermott et al., 42nd EPS 2015, paper P1.118.
[4] P. Mantica et al., Phys. Plasmas 17, 092505 (2010).
[5] S. Yang, private comm., APTWG Int. Conf., Seoul 2016.
[6] A.G. Peeters et al., Nucl. Fusion 51, 094027 (2011).
[7] S.-P. Pehkonen, et al.,this conference, paper P2.011.
[8] C. Chrystal, et al., APS Conference, 2015, USA, paper CO6.00008.